CrossMark
click for updates

In situ controllable synthesis of cotton-like polyaniline nanostructures for a H$_2$O$_2$ sensor using an embedded three-electrode microfluidic chip†

Mojie Sun,[a] Guoqing Song,[ab] Jingjing Liu,*[b] Hongmei Chen[b] and Fuqiang Nie*[b]

A robust embedded three-electrode microfluidic chip (TEMC) was designed for the *in situ* electrochemical synthesis of polyaniline (PANI) nanostructures. PANI doped with poly-vinylsulphonic acid (PVS) was electrochemically produced at a channel coated with a thin gold layer as the working electrode material. The resultant material formed a conductive monolithic PANI/PVS film with cotton-like nanostructures. The thickness and porosity of the polymeric material can be controlled by the polymerization conditions, *i.e.*, the number of potential cycles. Horseradish peroxidase (HRP) was subsequently electrostatically immobilized on the monolithic PANI/PVS film. This modified PANI/PVS/HRP material, obtained using a TEMC, showed a good linear response over a range of 0.01–0.6 mM and 1–60 mM for hydrogen peroxide detection and exhibited good reproducibility. This TEMC design could provide a simple and reliable approach for enzyme-based biosensor fabrication.

1. Introduction

As an important industrial material, H$_2$O$_2$ has been widely used in the food industry and is inevitably present in wastewater. Moreover, H$_2$O$_2$ is a product of enzymatic reactions in coupled enzyme systems. Unfortunately, H$_2$O$_2$ is extremely toxic to cellular life,[1] so the detection of H$_2$O$_2$ is of practical importance in pharmaceutical, clinical, industrial, environmental, and many other fields.[2] H$_2$O$_2$ has been detected by volumetric, colorimetric and chemiluminescence spectrometry,[3,4] but these techniques suffer from various interferences, long analysis times and usage of expensive reagents.

Since the concept of a micro-total analysis system (μ-TAS) was proposed by Manz *et al.* in 1990, significant advancements have been made towards the development of highly miniaturized analytical systems.[5] The advantages of a microfluidic platform are process integration, portability, small sample volumes, and high throughput analysis.[2] Particularly, electrochemical detection, *e.g.*, amperometry, has been perfectly incorporated into miniaturized analytical systems not only due to the inherent miniaturization and portability, but also due to the extremely low costs, low power requirements and compatibility with microfabrication technology.[6]

Amperometric biosensors made of organic conducting polymers, such as polyanilines (PANI), polyindoles, poly-carbazoles, polypyrroles and polythiophenes, have attracted tremendous interest for their simple operation, high operational stability, fast response, and very low limit of detection.[7] Among the polymers, PANI has been studied extensively owing to its easy preparation, low cost, performance, stability, and unique electrical, electrochemical and optical properties.[8,9] Furthermore, PANI is compatible with biological molecules in neutral aqueous solutions, so it is utilized as an excellent platform to immobilize biomolecules.[10] PANI can also act as a rapid electron mediator due to its excellent conductivity and electroactivity.[11,12] Therefore, PANI is employed in the most promising electrochemical biosensor applications.[13] In general, amperometric biosensors are composed of a base electrode substrate coated with a mediator, such as a conducting polymer film and an immobilized biomolecule, *e.g.*, HRP.[14] The polymer, PANI, can be electrochemically synthesized through galvanostatic, potentiostatic or potentiodynamic methods, which provide the potential to incorporate a wide range of dopants into the formation of the PANI film and provide good control of the thickness to improve the detection performance. However, there are many efforts focused on the study of PANI thin film fabrication on an electrode surface reported in the literature.[13,15] Among the applications of PANI films, thickness control has become more important in biosensors. For example, the electron transport efficiency is higher at thinner PANI thicknesses, which can enhance the lower limit of detection. On the other hand, more enzyme can be immobilized at thicker PANI thicknesses to provide a higher limit of detection. Therefore, it is necessary to control the PANI thickness for its real applications.

[a]*Department of Chemical Engineering, Northeast Electric Power University, Jilin, China. E-mail: smoj@sina.com*

[b]*Division of Nanobionic Research, Suzhou Institute of Nano-Tech and Nano-Bionics, Chinese Academy of Sciences, Suzhou, China. E-mail: fqnie2012@sinano.ac.cn; jjliu2015@sinano.ac.cn*

In this study, an embedded three-electrode microfluidic chip (TEMC) is proposed and demonstrated, which integrates three electrodes on a chip-scale for *in situ* electrochemical polymerization. By adjusting the polymerization conditions, a controllable monolithic PANI film can be fabricated and polymerized, and exhibits cotton-like nanostructures. The feasibility of using a TEMC for an HRP-H_2O_2 sensing device is demonstrated by amperometric detection. The experimental results indicate that it has a good reproducibility and long-term stability. This robust TEMC with cotton-like PANI nanostructures can be utilised in widespread applications, such as in chip-based biosensors, electrochromatography[16] and capacitors.[17]

2. Experimental section

2.1 Materials and methods

Materials and instruments. Aniline (99%), agarose and H_2O_2 solution (30%, v/v) were purchased from Sinopharm Chemical Reagent Co. Ltd., China. Poly(vinylsulfonic acid, sodium salt) (PVS, 25 wt% in water), horseradish hydrogen peroxide enzyme (HRP, 200 U per mg), and Pt and Ag wires of 0.5 mm lengths were obtained from Sigma-Aldrich Co., USA. PVDF membrane (no. HVLP2932A, pore size of filter: 0.45 μm) and inert acrylic pressure-adhesive polyester film (no. ARcare®8890) were purchased from Merck Millipore Ltd., Ireland and Adhesives Research Inc., Ireland, respectively. Other chemicals were of analytical grade and were used without further purification.

Phosphate buffered saline (PBS, pH = 6.8) was prepared using 0.1 M phosphate buffer, 0.137 M NaCl, and 2.7 mM KCl. The deionized water (resistance > 18 MΩ cm^{-1}) was treated by a Milli-Q system (model: Simplicity direct Q3 UV, Merck Millipore Ltd., Germany).

The morphology and composition of the synthesized PANI were characterized using a scanning electron microscope (SEM) (Quanta 250 FEG, FEI Co. Ltd., USA). Electrochemical measurements were performed using a workstation (model: CHI 660e, CH Instruments, Inc. USA) at room temperature.

Fabrication of the Ag/AgCl reference electrode. 0.9 g of agarose was added to 25 mL of 3.5 M KCl solution, and then the mixture was heated to form a high salinity solution. A Ag wire with a 0.5 mm diameter was polished using sand paper, and then dipped into a 0.1 M HCl solution. It was connected to the electrochemical workstation as an anode under a potential of 5 V for 15 min of electrochemical treatment. Finally, the wire was dipped into the high salinity solution for 5 to 10 seconds, and then taken out and cooled at room temperature to form a gel membrane on the surface. Therefore, this Ag/AgCl material can be used as a reference electrode (RE) and was ready for use in this study.

Fabrication of the chip-based electrochemical polymerization system. The chip has a sandwich structure as shown in Fig. 1, and the mockup and setup can be seen in Fig. S1 (ESI†). The WE lies on the bottom sheet and the CE and RE are embedded in the top sheet. The top sheet and bottom sheet are separated by an adhesive film, and the chamber position is replaced by a PVDF membrane. The application of a PVDF membrane played a crucial role in these embedded three
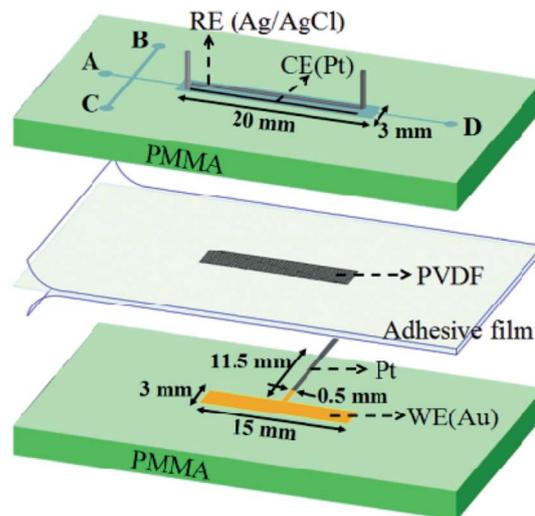

Fig. 1 Schematic diagram of the TEMC (A: inlet for solution; B: inlet for PBS and HRP solutions; C: inlet for air; D: outlet).

electrodes for *in situ* chip electropolymerization. Firstly, the polymerization mixture can penetrate through the PVDF membrane due to the porosity and hydrophilicity of the membrane. Secondly, the PVDF membrane was a physical barrier which protected the PANI from contact with the CE and RE during growth. Therefore, the process of electropolymerization could be precisely controlled. When the formation of polymer was from the bottom to the top, the pore size of the polymer structure could be controlled by adjusting the polymerization time. The controllability of pore size would benefit its application in chip-based electrochromatography. Finally, the top PMMA sheet was pasted with the bottom PMMA sheet by using a piece of inert acrylic pressure-adhesive polyester film, and then the TEMC was connected with the electrodes of the electrochemical workstation for polymerization.

Electropolymerization of aniline. A mixture of 185 μL of aniline, 2 mL of PVS and 7.8 mL of HCl (1 M) was degassed under nitrogen for 10 min, and continuously pumped through the inlet for the precursor solution (denoted as A in Fig. 1) with a flow velocity of 40 μL min^{-1} (all the processes were conducted at this flow rate). The potential range of the cyclic voltammogram was from −0.2 to 1.0 V with a scanning rate of 100 mV s^{-1} and a cycling range of 5–60. Aniline was successively grown on the gold surface using the CV model and eventually formed PANI cotton-like nanostructures on the surface. PBS buffer (degassed for 10 min under nitrogen) was continuously pumped through the inlet for the PBS and HRP solutions (denoted as B in Fig. 1) to clean the chamber, and then the PANI film was reduced at −500 mV (*vs.* Ag/AgCl) for 1500 s in the *i–t* mode with a sample interval of 0.5 s. PBS buffer was removed from the inlet for air (denoted as C in Fig. 1) and then the HRP solution (1 mg mL^{-1}, in PBS) was quickly pumped through B. Therefore, the oxidized reaction was performed immediately at 700 mV (*vs.* Ag/AgCl) for 1500 s. In the oxidation process, HRP would electrostatically attach to the PANI surface.[18] Eventually, the TEMC was completed as a H_2O_2 biosensor for use in subsequent experiments.

3. Results and discussion

3.1 Characterization of the PANI modified electrode

The mixture of aniline, PVS and HCl was utilized to investigate *in situ* electropolymerization within the TEMC platform. The PANI thin-film can be electrochemically deposited on electrode surfaces using galvanostatic, potentiostatic or potentiodynamic methods. Among them, the formation of a furrowed PANI thin-film was more homogeneous and adhered on the electrode surface using the potential-scanning method.[19] PANI thin-films produced in non-acidic media generally did not keep their conductive characterization, which is a severe problem for the development of a PANI/enzyme-based biosensor. Therefore, the electropolymerization process had to be carried out in the presence of a dopant like PVS.[20–22] The role of PVS was to maintain the electrical neutrality in the oxidized form of the polymer. Also, PVS can increase the structural stability and conductivity of the polymer over a broader range of pH values.[23]

A mixture of aniline/PVS/HCl was used for all electropolymerization on a gold surface as the WE material by CV at 100 mV s^{-1} as shown in Fig. 2(a). The CV was typical for PANI/PVS, with three oxidation peaks (A, B and C) and three corresponding reduction peaks (a, b and c) that are comparable to those reported in the literature.[24] The polymerization current responses increased with the number of potential cycles, which confirmed that the polymer was conducting and electroactive and indicated that polyaniline had aggregated on the gold surface. It was also found that shifts in peak potentials started to occur after a number of potential cycles, which increased the electrode resistance due to the formation of a thicker PANI/PVS film.[25]

Currently, most of the research on PANI electropolymerization has focused on the polymer thin-film on the electrode surface. Herein, we have proposed and demonstrated a different approach to fabricate *in situ* polymerized monolithic PANI/PVS nanostructures with controllable thickness. It is well known that the polymer thickness was increased by successive potential cycles. To investigate the effects of the number of potential cycles on the polymer thickness, the initial depth of the channel with a gold thin-film as the polymerization site was designed to be 40 μm, which provided enough space for polymer growth from bottom to top in the TEMC. Fig. 2(b) shows the relationship between the number of potential cycles and the thickness of the electro-polymerized PANI/PVS film. Over the range of 5 to 60 potential cycles, the polymer thickness increased from 1.7 to 26.4 μm gradually. Furthermore, the morphology of the PANI/PVS film became more porous, which was caused by the rough contact surface during polymerization by increasing the number of potential cycles as shown in the SEM images in Fig. 2(b). The experimental results indicated that the thickness of the PANI/PVS film was definitely controllable. Furthermore, high quality SEM graphs can be seen in the ESI.†

In order to practically evaluate the PANI film developed here, the PANI/PVS film that was used to immobilize HRP in order to realize H$_2$O$_2$ detection was designed as follows. Multi-potential step chronoamperometric measurements were employed to
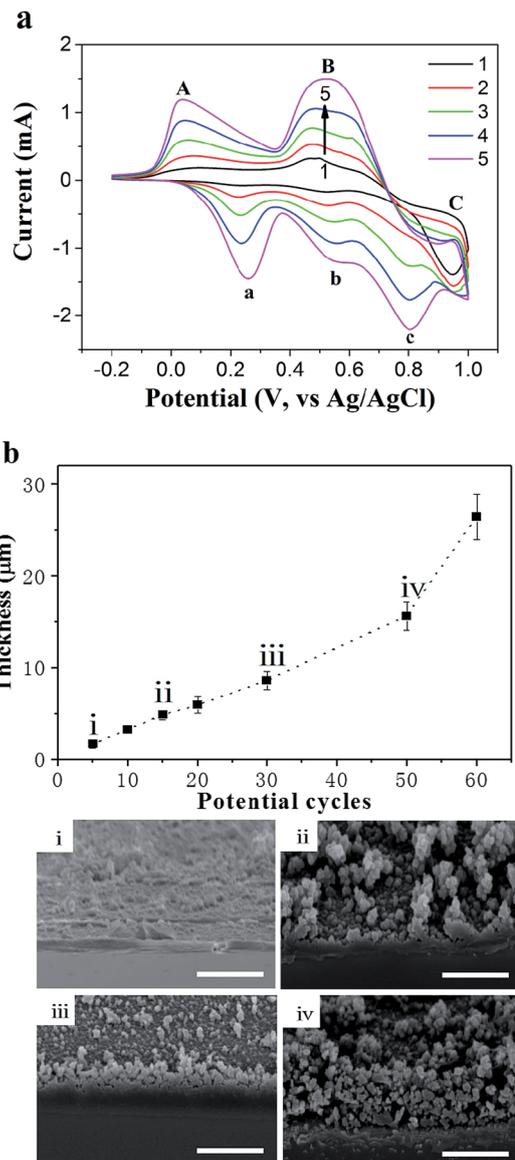

Fig. 2 (a) Five cyclic voltammograms of a PANI/PVS film fabricated on a gold surface as the WE material, with a scanning rate of 100 mV s^{-1}, where A, B, and C are the anodic peaks of the oxidation of PANI, emeraldine, and pernigraniline, respectively, and a, b, and c are the corresponding reduction peaks of A, B, and C. (b) The relationship between the potential cycles and the PANI/PVS film thickness. Flow velocity 40 μL s^{-1}; the thicknesses of the films are shown in the SEM images (i–iv) that correspond to different numbers of potential cycles. The scale bars correspond to 10 μm.

study the effects of the number of potential cycles on the redox switching of the PANI/PVS thin-film to determine the applied number of potential cycles in the fabrication of the biosensor. Fig. 3 shows the chronoamperometric transients upon oxidation (1.0 V) and reduction (0.0 V) of the polymer. It is clear from the results of Fig. 2(b) that more potential cycles resulted in a thicker polymer film, and the results of Fig. 3 show that thicker films exhibit a slower redox switching phenomenon. Grennan *et al.* studied the influence of the thickness of the PANI film on a variety of amperometric sensor characteristics and
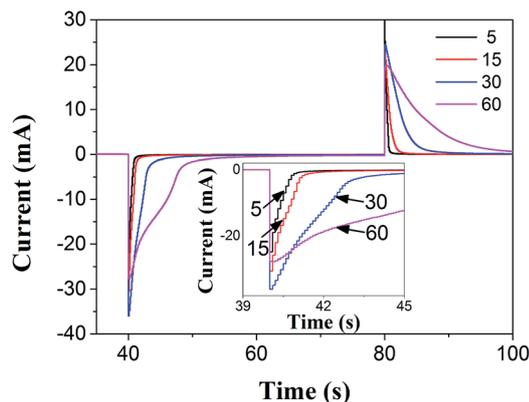
Fig. 3 Effect of the number of potential cycles on the redox switching of the PANI/PVS film.

found that increasing the polymer thickness resulted in increasing response times of the sensors as well as background and charging currents; the optimal thickness of the thin-film was found to be 13.7 µm.[26] There is a tradeoff between polymer thickness and electron transfer properties owing to the fact that a thicker polymer film will hinder the electron transfer properties between the electrode surface and the bulk solution. A thinner polymer film would be preferable for sensor applications.[27] Morrin *et al.* found that the current response decreased in their nanoscale PANI/DBSA biosensor above 30 cycles.[28] Therefore, for the following HRP-based biosensor application, the depth of the channel as the electropolymerization site was designed as ~10 µm, with 30 potential cycles as shown in Fig. 2(b), which ensured the formation of the monolithic polymer.

3.2 Characteristics of TEMC-based H_2O_2 biosensor

According to the basic amperometric procedure mentioned above, 1 mg mL^{-1} HRP was electrostatically immobilized onto the monolithic polymer to realize the function of H_2O_2 sensing. Fig. 4 presents a schematic diagram of the electron transfer mechanism in the enzymatic reaction of the PANI/HRP based H_2O_2 biosensor. The whole reaction was performed while the PANI was oxidized by H_2O_2 with the electro-catalysis of HRP.

Heme, acting as an active agent in the HRP enzyme, contains Fe^{3+} and a neutral porphyrin ring (P^0). HRP is activated at 30 °C over the environmental pH range of 6–8. In general, the HRP immobilized electrode electrocatalytic reduction of H_2O_2 can be expressed as follows.

$$HRP(Fe^{3+},P^0) + H_2O_2 \rightarrow \text{compound I } (Fe^{4+},P^{\bullet}) + H_2O \quad (1)$$

$$\text{Compound I } (Fe^{4+},P^{\bullet}) + AH_2 \rightarrow \text{compound II } (Fe^{4+},P^0) + AH^{\bullet} \quad (2)$$

$$\text{Compound II } (Fe^{4+},P^0) + AH_2 \rightarrow HRP(Fe^{3+},P^0) + AH^{\bullet} \quad (3)$$

HRP contains Fe^{3+} and a neutral porphyrin ring (P^0). In the first stage of the cycle reaction, Fe^{3+} and P^0 in the prosthetic group of HRP provide two electrons and form the intermediate compound I. In the second stage, the electron transfer is from AH_2 to compound I, which forms compound II and the radical reaction product of $AH^{\bullet}$. Finally, compound I and compound II are reduced with the adsorption of a proton. For this electro-catalyzed reaction, the potential of the reduction current of H_2O_2 is the same as the oxidation potential of compound II. As molecular oxygen is competitive in the ferrous oxide enzyme dioxygen reaction, it is necessary to avoid the impact of dissolved oxygen in the ampere test.

The surface of the film is the outermost part that connects with the external environment in the catalyst reaction, and the nanostructure enables different electronic and catalyst properties to those of bulk materials.[29] Fig. 5(a) shows the surface morphology of the PANI/PVS/HRP film synthesized at the channel by 30 potential cycles. The polymer layer exhibited a monolithic structure composed of continuous cotton-like nanostructures with mesopores on the surface as shown in Fig. 5(b). The porous surface enables the film to exhibit good adsorption and have a wide reaction area, both of which have a positive influence on detection.

In order to further investigate the characterization of the TEMC-based H_2O_2 biosensor for the detection of different H_2O_2 concentrations, we measured the amperometric response to H_2O_2 using a self designed continuous flow detection system, which can be seen in Fig. S2 (ESI†). Fig. 6(a) shows the calibration curve of the TEMC-based H_2O_2 biosensor and indicates a linear range of the PANI/PVS/HRP electrode response from
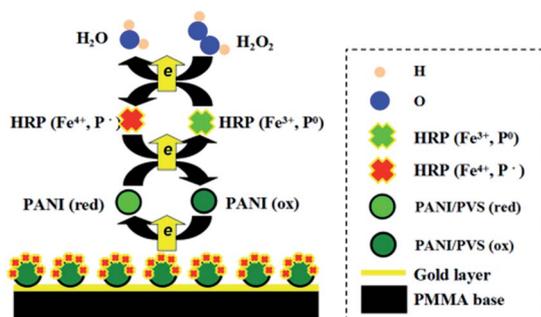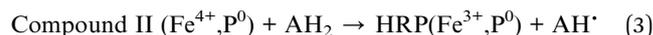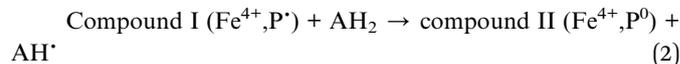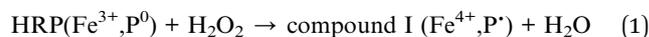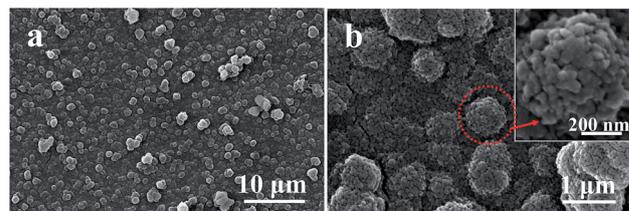

Fig. 4 Schematic diagram of the electron transfer mechanism in the enzymatic reaction of the PANI/HRP based H_2O_2 biosensor.

Fig. 5 SEM images of the PANI/PVS/HRP thin-film (fabricated by 30 potential cycles with a flow rate of 40 µL min^{-1}) at (a) low magnification and (b) high magnification, inset is the magnification of the dashed circle part.
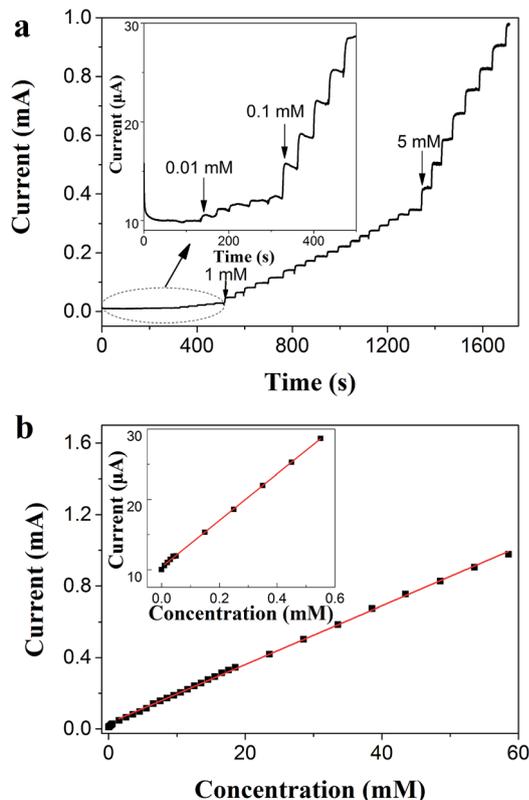
a

b

Fig. 6 (a) Amperometric response to H_2O_2 with different concentrations at a potential of −0.2 V. The inset shows the magnification of the curve highlighted by the dashed circle; (b) calibration plot of the relationship between the response current and the H_2O_2 concentration. The inset shows the low concentration region (between 0 and 0.6 mM).

0.01–0.6 mM $[Y\,(\text{mA}) = 0.010 + 0.033X\,(\text{mM}), R_2 = 0.99973]$ and 1–60 mM $[Y\,(\text{mA}) = 0.032 + 0.016X\,(\text{mM}), R_2 = 0.99931]$ as shown in Fig. 6(b). The detection limit was estimated as 1.49 μM (S/N = 3). At low H_2O_2 concentrations, the substrate *i.e.*, H_2O_2 is depleted rapidly as it is converted into product by the catalytic action of PANI/PVS/HRP at the electrode surface, thus resulting in a high sensitivity response. When the H_2O_2 concentrations increase, the nano-pores supply substrate over a larger time window during the proceeding reaction, and the possibility of reaction products obstructing the electrode surface increases, which results in a lower sensitivity.[30]

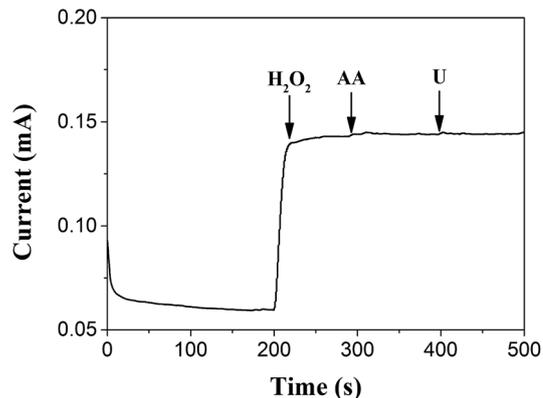The performance of the TEMC-based H_2O_2 biosensor compared to those of previous H_2O_2 sensors based on various

Fig. 7 Amperometric response of the PANI/PVS/HRP electrode to 2 mM H_2O_2, 20 mM ascorbic acid (AA) and 20 mM urea (U), respectively, at a potential of −0.2 V.

PANI/HRP composites is summarized in Table 1. The linear range of the TEMC-based H_2O_2 biosensor in the upper limit of detection was not comparable to the best result summarized in Table 1. However, the TEMC-based H_2O_2 biosensor represents two linear ranges, with amperage responses over a wider order of magnitude range from 10^{-2} to 10^2 mM, which makes it suitable for use in extensive applications. Furthermore, the performances of the reported sensors are difficult to compare directly due to the use of additional mediators and different working potentials.

Fig. 7 shows the current response to electroactive compounds of 20 mM ascorbic acid (AA) and urea (U) using the TEMC-based H_2O_2 biosensor at a potential of −0.2 V during the measurement of 2 mM H_2O_2. The amperometric response to H_2O_2 is not influenced significantly. Such behavior indicated that the activity towards H_2O_2 cannot be impacted significantly by the interferences. This can be attributed to the specificity of horseradish peroxidase.

The reproducibility was estimated by successive determinations of 2 mM H_2O_2 with the same TEMC-based H_2O_2 biosensor; the peak patterns of the amperometric response were kept similar for five consecutive injections and the relative standard deviation (RSD) was better than 5%, which indicated that the system had a good reproducibility and was quite credible. After 50 successive assays, the response remained at 88% of the initial response. This may be a result of the *in situ* electrochemical polymerization, because the configuration of the

Table 1 Comparison of the performances of various PANI/HRP-based H_2O_2 sensors

Electrode materials	Detection limit/μM	Liner range/mM	Ref.
PANI/single-wall carbon nanotubes	0.9	2.5–50.0	31
Ag nanoparticle/PANI/graphene composites	30	0.25–2.25	32
PANI nanotubes	1.5	1–200	33
Perchlorate/PANI film	—	3–136	34
Gold doped polyaniline composite	1.6	0.03–2	35
Pt nanoparticles doped PANI nanofiber membrane	2.8	7–14	36
Cotton-like PANI/PVS nanostructure film	1.5	0.01–0.6 and 1–60	This work

channel increased the stability of the polymer and the nano-structure was propitious towards the attachment of HRP.

4. Conclusions

In conclusion, an *in situ* electrochemical polymerization of a PANI/PVS film with cotton-like nanostructures using TEMC was proposed and demonstrated. The thickness of the PANI/PVS film could be controlled by adjustment of the number of potential cycles, and the film also exhibited good conduction and electroactivity. The polymer film was made porous by increasing the number of potential cycles. The relevant functions were realized by immobilizing HRP on the PANI/PVS film surface. This modified PANI/PVS/HRP material exhibits two linear responses over the ranges of 0.01–0.6 mM and 1–60 mM for hydrogen peroxide detection. The broad linear detection range, low detection limit, high sensitivity and acceptable reproducibility of the material would make it capable of acting as a good alternative for H_2O_2 sensors.

Acknowledgements

References

1 Q. Shi, Y. Song, C. Zhu, H. Yang, D. Du and Y. Lin, *ACS Appl. Mater. Interfaces*, 2015, **7**, 24288–24295.

2 T. Ruzgas, E. Csoregi, J. Emneus, L. Gorton and G. MarkoVarga, *Anal. Chim. Acta*, 1996, **330**, 123–138.

3 S. G. Rhee, T. S. Chang, W. Jeong and D. Kang, *Mol. Cells*, 2010, **29**, 539–549.

4 A. Roda, M. Mirasoli, E. Michelini, M. Di Fusco, M. Zangheri, L. Cevenini, B. Roda and P. Simoni, *Biosens. Bioelectron.*, 2016, **76**, 164–179.

5 A. Manz, N. Graber and H. M. Widmer, *Sens. Actuators, B*, 1990, **1**, 244–248.

6 V. N. Goral, N. V. Zaytseva and A. J. Baeumner, *Lab Chip*, 2006, **6**, 414–421.

7 K. Lee, S. Cho, S. H. Park, A. J. Heeger, C. W. Lee and S. H. Lee, *Nature*, 2006, **441**, 65–68.

8 C. Sheng and S. Gang, *ACS Appl. Mater. Interfaces*, 2013, **5**, 6473–6477.

9 L. Tiggemann, S. Ballen, C. Bocalon, A. M. Graboski, A. Manzoli, P. S. D. P. Herrmann, J. Steffens, E. Valduga and C. Steffens, *J. Food Eng.*, 2016, **180**, 16–21.

10 J. Liu, S. Lu, X. Liang, Q. Gan, Y. Wang and H. Li, *J. Electroanal. Chem.*, 2016, **764**, 15–22.

11 B. Yu, J. Song, Y. Mao, D. Han, F. Yang, N. Li and A. Ivaska, *Electroanalysis*, 2011, **23**, 878–884.

12 L. Chen, Z. Su, X. He, Y. Liu, C. Qin and Y. Zhou, *Electrochem. Commun.*, 2012, **15**, 34–37.

13 C. Dhand, M. Das, M. Datta and B. D. Malhotra, *Biosens. Bioelectron.*, 2011, **26**, 2811–2821.

14 S. Bao, M. Du, M. Zhang, H. Zhu, P. Wang, T. Yang and M. Zou, *Chem. Eng. J.*, 2014, **258**, 281–289.

15 A. T. Lawal and G. G. Wallace, *Talanta*, 2014, **119**, 133–143.

16 J. Zhang, W. Zhang, T. Bao and Z. Chen, *J. Chromatogr. A*, 2014, **1339**, 192–199.

17 Y. E. Miao, W. Fan, D. Chen and T. Liu, *ACS Appl. Mater. Interfaces*, 2013, **5**, 4423–4428.

18 K. Grennan, A. J. Killard and M. R. Smyth, *Electroanalysis*, 2005, **17**, 1360–1369.

19 Q. Xu, J. J. Zhu and X. Y. Hu, *Anal. Chim. Acta*, 2007, **597**, 151–156.

20 N. Prabhakar, G. Sumana, K. Arora, H. Singh and B. D. Malhotra, *Electrochim. Acta*, 2008, **53**, 4344–4350.

21 N. C. S. Vieira, E. G. R. Fernandes, A. D. Faceto, V. Zucolotto and F. E. G. Guimarães, *Sens. Actuators, B*, 2011, **160**, 312–317.

22 F. Arslan, S. Ustabaș and H. Arslan, *Sensors*, 2011, **11**, 8152–8163.

23 G. Li, Y. Wang and H. Xu, *Sensors*, 2007, **7**, 239–250.

24 L. Shahhosseini, M. R. Nateghi, M. Kazemipour and M. B. Zarandi, *Prog. Org. Coat.*, 2015, **88**, 272–282.

25 M. C. Santos, M. L. Munford and R. F. Bianchi, *Mater. Sci. Eng., B*, 2012, **177**, 359–366.

26 K. Grennan, A. J. Killard, C. J. Hanson, A. A. Cafolla and M. R. Smyth, *Talanta*, 2006, **68**, 1591–1600.

27 S. K. Bhardwaj, N. Bhardwaj, G. C. Mohanta, P. Kumar, A. L. Sharma, K. H. Kim and A. Deep, *ACS Appl. Mater. Interfaces*, 2015, **7**, 26124–26130.

28 A. Morrin, O. Ngamna, A. J. Killard, S. E. Moulton, M. R. Smyth and G. G. Wallace, *Electroanalysis*, 2005, **17**, 423–430.

29 A. N. Shipway, E. Katz and I. Willner, *ChemPhysChem*, 2000, **1**, 18–52.

30 X.-x. Dong, M.-y. Li, N.-n. Feng, Y.-m. Sun, C. Yang and Z.-l. Xu, *RSC Adv.*, 2015, **5**, 86485–86489.

31 N. Tang, J. Zheng, Q. Sheng, H. Zhang and R. Liu, *Analyst*, 2010, **136**, 781–786.

32 S. Li, J. Xiong, J. Shen, Y. Qin, J. Li, F. Chu, Y. Kong and L. Deng, *J. Appl. Polym. Sci.*, 2015, **132**, 42409.

33 A. Jabłońska, M. Gniadek and B. Pałys, *J. Phys. Chem. C*, 2015, **119**, 12514–12522.

34 P. R. Solanki, A. Kaushik, A. A. Ansari, G. Sumana and B. D. Malhotra, *Polym. Adv. Technol.*, 2011, **22**, 903–908.

35 P. M. Ndangili, T. T. Waryo, M. Muchindu, P. G. L. Baker, C. J. Ngila and E. I. Iwuoha, *Electrochim. Acta*, 2010, **55**, 4267–4273.

36 S. Chen, P. Fu, B. Yin, R. Yuan, Y. Chai and Y. Xiang, *Bioprocess Biosyst. Eng.*, 2011, **34**, 711–719.